

Breather—kink-antikink-pair conversion in the driven sine-Gordon system

P. S. Lomdahl and O. H. Olsen*

Center for Nonlinear Studies, Los Alamos National Laboratory, Los Alamos, New Mexico 87545

M. R. Samuelsen

Physics Laboratory I, The Technical University of Denmark, DK-2800 Lyngby, Denmark

(Received 15 July 1983)

Breather excitations in the sine-Gordon equation influenced by constant driving forces are investigated—large driving forces cause the breather to split into a $k\bar{k}$ (2π kink— 2π antikink) pair while for small driving forces the breather excitations enter stationary modes. A perturbation method and a potential-energy argument yields expressions for the threshold for breather decomposition. Good agreement between theory and numerical results is found when the initial phase (θ) of the breather is either 0 or π . For $\theta \cong \pi/2$ and $\theta \cong 3\pi/2$ the deviation gets larger.

I. INTRODUCTION

The study of nonlinear wave phenomena in quasi-one-dimensional systems has recently drawn considerable theoretical and experimental effort because of the relative ease with which current theories can be tested.¹ In particular the Josephson junctions modeled by the perturbed sine-Gordon equation with appropriate boundary conditions is remarkable—most of the experimental findings are explained in the framework of the model.^{2,3} Further, the sine-Gordon equation has been used to model, e.g., propagation of ultrashort optical pulses and propagation of crystal dislocations.⁴

The pure sine-Gordon equation possesses the remarkable soliton and antisoliton solutions (2π -kink solutions) and the so-called breather solution which can be viewed as a bound state of a soliton and an antisoliton. The breather solution itself is a soliton solution. Unlike the 2π -kink solutions, the breather need not require an activation energy because its rest energy can range from 0 to $2E_0$, where E_0 is the rest energy of the kinks and antikinks. Further, the breathers' internal degree of freedom increases their physical potential.

The perturbed sine-Gordon equation, where the perturbing terms represent dissipative effects, energy input, and various kinds of impurities has been analyzed by several authors.^{5–7} Specific analyses of breather solutions to the perturbed sine-Gordon equation have been performed by Scott,⁸ Inoue and Chung,⁹ and Inoue.¹⁰ In Ref. 8 the perturbation scheme outlined in Ref. 7 is used to calculate the dynamic behavior of a moving breather under influence of dissipative and energy supplying terms in the sine-Gordon equation while in Refs. 9 and 10 the breather is shown to dissociate into a kink-antikink pair ($k\bar{k}$) when influenced by large driving forces.

In the present paper we examine the influence of a driving force on a breather excitation. In the presence of damping a kink and an antikink can annihilate each other. During this process an intermediate breather state is formed, but it collapses into plasmons. In the presence of a driving force, it is possible for breathers to convert into

a $k\bar{k}$ pair (i.e., 2π kink— 2π antikink pair).^{9–11} Application of a perturbation method and a potential-energy argument yield expressions describing the borderline between regions where breathers decompose and enter breatherlike modes, respectively. However, numerical experiments show that the breather conversion depends strongly on the initial phase of the breather—the expressions only agree with the experiments in half the range of the initial phase of the breather. Further, numerical investigations show that breathers influenced by a driving force less than the threshold value enter stationary modes.

The outline of the paper is as follows. In Sec. II we derive expressions for the threshold value of the driving force η_{cr} versus the initial frequency ω_B of the breather as well as an expression for the frequency of a breather influenced by driving forces less than η_{cr} . Section III contains comparisons between analysis and numerical experiments. Finally in Sec. IV we summarize and conclude the paper.

II. ANALYSIS

In this section we derive expressions for the threshold value of the driving force η_{cr} versus the initial frequency ω_B of the breather. Firstly, a perturbation approach is used to obtain expressions for η_{cr} vs ω_B and for the frequency of the breather influenced by a driving force less than η_{cr} . Secondly, an instructive energy argument is used to derive a similar expression for η_{cr} vs ω_B .

The equation in question is the perturbed sine-Gordon equation

$$\phi_{xx} - \phi_{tt} = \sin\phi + \eta, \quad (1)$$

where time and space are denoted t and x , respectively. The term η is the driving force. The Hamiltonian for the pure sine-Gordon equation [Eq. (1) with $\eta=0$] is

$$H(t) = \int \left[\frac{1}{2}\phi_x^2 + \frac{1}{2}\phi_t^2 + (1 - \cos\phi) \right] dx. \quad (2)$$

Differentiation of (2) and insertion of (1) yield⁷

$$\dot{H}(t) = -\eta \int \phi_t dx. \quad (3)$$

The breather solution to the pure sine-Gordon equation is given by

$$\phi(x,t) = 4 \tan^{-1} \left[\frac{(1-\omega_B^2)^{1/2}}{\omega_B} \sin[\omega_B(t-t_0)] \right. \\ \left. \times \operatorname{sech}[(1-\omega_B^2)^{1/2}(x-x_0)] \right]. \quad (4)$$

Here x_0 and $\omega_B t_0 = \theta$ is the initial position and phase of the breather, ω_B is the initial frequency. The traveling breather solution is obtained by Lorentz transformation of the solution (4).

In order to determine the time evolution of the breather it is necessary to calculate the integral in Eq. (3). This has

$$H(t) = H_B - \frac{4\pi\eta}{(1-\omega_B^2)^{1/2}} \ln \left[\frac{(1-\omega_B^2)^{1/2}}{\omega_B} \sin[\omega_B(t-t_0)] + \left[1 + \frac{1-\omega_B^2}{\omega_B^2} \sin^2[\omega_B(t-t_0)] \right]^{1/2} \right], \quad (7)$$

where H_B is given by (6).

Now, a condition for conversion of a breather into a $k\bar{k}$ pair can be obtained. If the energy (7) exceeds the rest energy of a 2π kink and a 2π antikink, it becomes energetically possible for the breather to convert into a $k\bar{k}$ pair. Thus an expression for the lower bound of the critical value of the driving force η_{cr} versus the initial frequency ω_B is

$$\eta_{cr} = \frac{4}{\pi} \frac{[1 - (1-\omega_B^2)^{1/2}](1-\omega_B^2)^{1/2}}{\ln \left[\frac{1}{\omega_B} [1 + (1-\omega_B^2)^{1/2}] \right]}. \quad (8)$$

We stress that the calculations above have been performed under the restrictive assumption that ω_B and t_0 are independent of time. An approximate expression for the frequency of a breather influenced by a driving force less than the threshold force can be found by assuming that an expression similar to Eq. (6) holds even when ω_B is a function of time: $\omega(t)$. Differentiating Eq. (6) with respect to time then yields the following:

$$-16\omega(1-\omega^2)^{1/2}\dot{\omega} \cong -16\omega_B(1-\omega_B^2)^{1/2}\dot{\omega}.$$

By insertion of this approximation in Eq. (5) and by integration we get

$$\omega = \omega_B + \frac{\pi\eta}{4\omega_B} \ln \left[\frac{(1-\omega_B^2)^{1/2}}{\omega_B} \sin[\omega_B(t-t_0)] + \left[1 + \frac{1-\omega_B^2}{\omega_B^2} \sin^2[\omega_B(t-t_0)] \right]^{1/2} \right]. \quad (9)$$

This expression reflects the fact that a positive (negative) driving force accelerates a 2π kink (2π antikink) to the right and a 2π antikink (2π kink) to the left. Therefore, the part of the period where the force tends to split the breather is longer than the part where the driving force and the breather mechanism work together.

not been performed in general because ω_B and t_0 are functions of time, but assuming ω_B and t_0 independent of time, insertion of (4) into (3) and integrating we get

$$\dot{H}(t) = -4\pi\eta \frac{\cos[\omega_B(t-t_0)]}{\left[1 + \frac{1-\omega_B^2}{\omega_B^2} \sin^2[\omega_B(t-t_0)] \right]^{1/2}}. \quad (5)$$

The energy of a static breather solution to the pure sine-Gordon equation is given by⁸

$$H_B = 16(1-\omega_B^2)^{1/2}. \quad (6)$$

Further, the rest energy of a 2π kink is 8. Integration of (5) yields the energy $H(t)$ of the breather

Finally in this section we present an analysis for breather conversion into a $k\bar{k}$ pair based on a potential energy argument.¹¹ In Fig. 1 we have sketched the potential $V(\phi) = 1 - \cos\phi + \eta\phi$. If a breather is oscillating around a ground state

$$\phi_0 = -\sin^{-1}\eta \pmod{2\pi} \quad (10)$$

which is the trivial solution to Eq. (1), it is clear that if it can overcome the energy gap ΔV , it can reach the lower ground state $\phi_2 = \phi_0 + 2\pi$. But by doing so it breaks up into a $k\bar{k}$ pair (cf. the unperturbed case). The energy gap is given by

$$\Delta V = V(\phi_1) - V(\phi_0) \\ = 2[(1-\eta^2)^{1/2} + \eta \sin^{-1}\eta] + \eta\pi, \quad (11)$$

where ϕ_1 is the unstable point $\phi_1 = \pi + \sin^{-1}\eta \pmod{2\pi}$. In the unperturbed case, the gap $\Delta V = 2$ while the energy required by the breather is 16. Assuming this ratio to be valid in the presence of the driving force, we get the relation

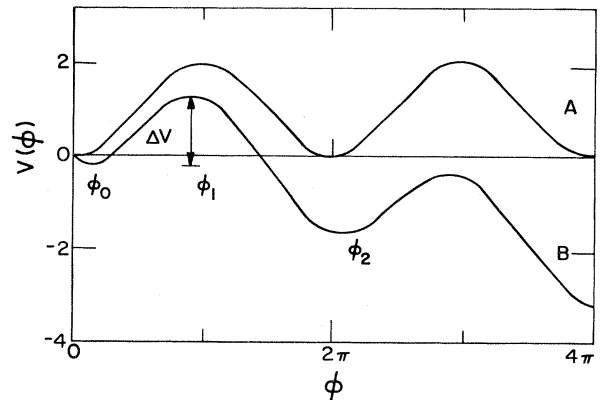


FIG. 1. Potential $v(\phi) = 1 - \cos\phi + \eta\phi$ drawn for (a) $\eta=0$ and (b) $\eta=-0.265$.

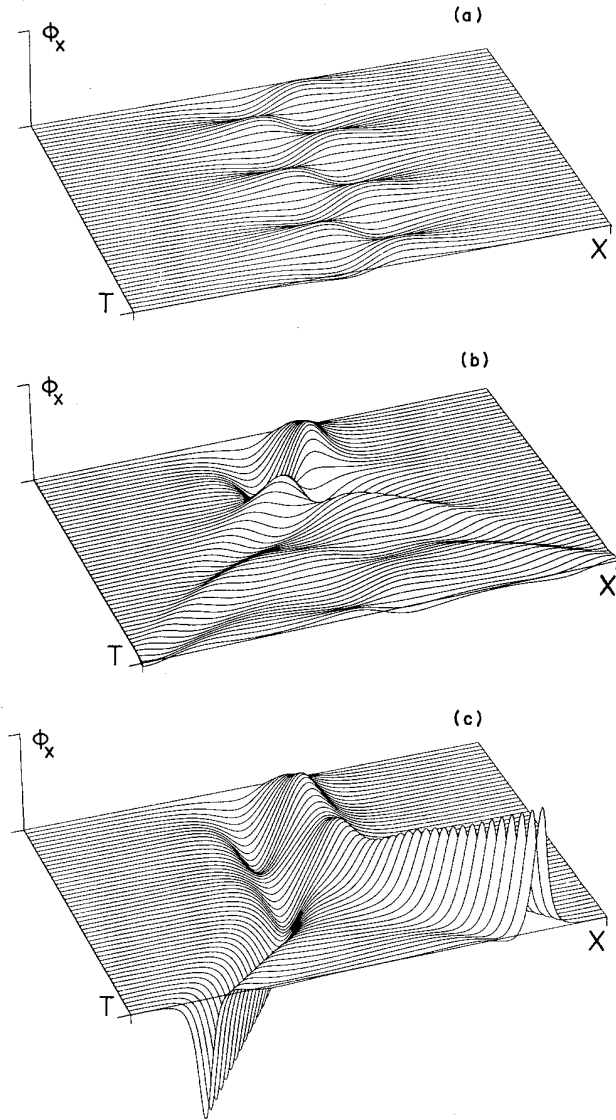


FIG. 2. Time evolution of breathers influenced by force terms. Parameter values are $\omega_B=0.8$, $t_0=0$, $\eta=0.1$ (a), $\eta=0.25$ (b), and $\eta=0.265$ (c). For the low value of the force (a) the breather almost immediately enters a stationary mode—only little radiation is observed, while for the value of the force in (b), just below the threshold value, the picture is different—much radiation is observed, see Fig. 3. In (c) the breather decomposes into a $k\bar{k}$ pair. The time evolution $0 < t < 25$ is shown.

$$16(1-\omega_B^2)^{1/2}/\Delta V(\eta_{cr}) = \frac{16}{2} \quad (12a)$$

or

$$(1-\omega_B^2)^{1/2} = (1-\eta_{cr}^2)^{1/2} + \eta_{cr} \sin^{-1} \eta_{cr} + \frac{\eta_{cr} \pi}{2} \quad (12b)$$

In the next section we compare the analyses in this section with numerical experiments.

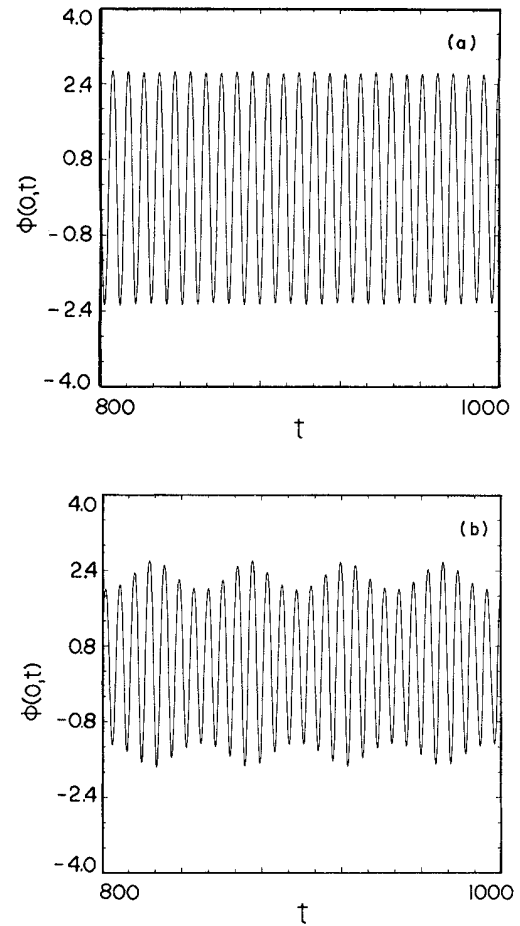


FIG. 3. Value of $\phi(0,t)$ (the point of symmetry) vs time. Parameter values as in Figs. 2(a) and 2(b). After transients the breathers enter stationary modes. For the higher value of the force (b) $\phi(0,t)$ is modulated.

III. NUMERICAL RESULTS AND COMPARISONS WITH ANALYSES

We solve the initial value problem Eq. (1) with outflow boundary conditions at $x = -15$ and 15 . In the expression $\phi(x,0)$ [Eq. (4)] for the initial profile we choose $x_0=0$ throughout this section. The numerical solutions are obtained by means of a computer program based on an implicit finite-difference method which is second order in both space and time.¹¹ Further, we choose the vacuum in the ground state,¹² i.e., $\phi(\pm\infty,t) = -\sin^{-1}\eta$. None of the results presented here were sensitive to this choice of vacuum [similar results were obtained with $\phi(\pm\infty,t)=0$].

In Fig. 2 we show the time evolution of a breather influenced by a force. The initial frequency of the breather is $\omega_B=0.8$ and the initial phase is $\theta=0$. In Figs. 2(a) and 2(b) the value of the force terms is below the threshold value. In Fig. 2(a) the breather almost immediately enters a stationary mode—only a small amount of radiation is observed. In Fig. 2(b) the value of the force term is just below the threshold value resulting in creation of radiation

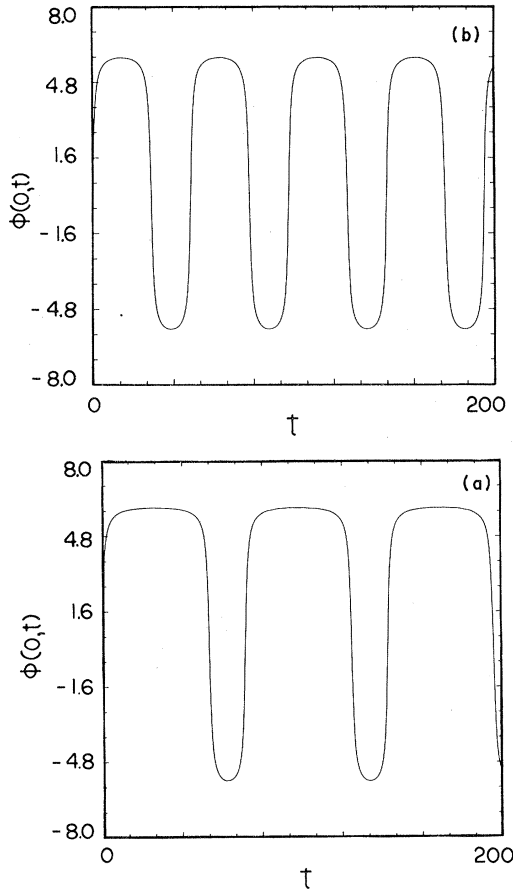


FIG. 4. Illustration of the breathers internal contraction and repulse forces. The point of symmetry $\phi(0,t)$ vs time. Parameter values are $\omega_B=0.1$, $t_0=0$, $\eta=0.0027$ (a), and $\eta=0.0015$ (b). The part of the period where the breather tends to dissociate is longest.

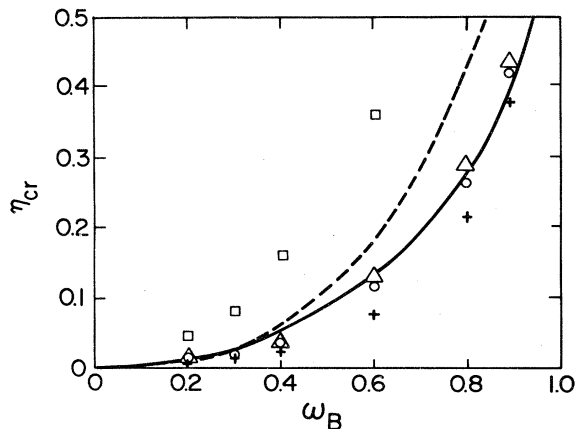


FIG. 5. Comparisons between the analytical expressions for the threshold force η_{cr} vs the initial frequency ω_B and numerical experiments. Solid lines represent the following analyses: The dashed curve is the perturbation analysis and the solid curve is the potential energy analysis. The points are numerically determined, $\theta=\omega_B t_0=0$ (\circ), $\pi/2$ (\square), π (\triangle), $\frac{3}{2}\pi$ ($+$). The dissociation depends strongly on the initial phase θ , see Fig. 6.

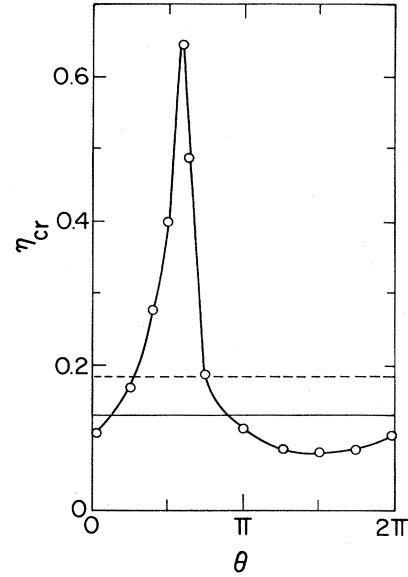


FIG. 6. Influence of the initial phase ($\theta=\omega_B t_0$) of the breather. The solid and dashed horizontal lines represent the energy and perturbation analysis, respectively—the solid curve is determined from numerical experiments. For $\omega_B t_0 \sim \pi/2$ the deviation from the analyses has a maximum resulting from the fact that the initial energy of the breather deviates most from the energy of the unperturbed breather.

before a stationary mode occurs, see Fig. 3. Finally in Fig. 2(c) the breather decomposes into a $k\bar{k}$ pair.

In Fig. 3 we show $\phi(0,t)$ (the point of symmetry) versus time for the situations shown in Figs. 2(a) and 2(b). After transients the breathers enter stationary modes—for the higher value of the force the mode is modulated. These examples illustrate the behavior of breathers below the threshold value: after transients stationary modes occur. This result has been predicted in Refs. 7 and 8 for $\omega \cong 1$ and $\eta \ll 1$ by application of a perturbation theory. In Fig. 4 we show how the force influences the stationary mode for small initial frequencies. The part of the period where the breather tends to dissociate is the longest—illustrating the internal contraction and repulse forces. The behavior of the breather in Fig. 4 is in qualitative agreement with Eq. (9).

Finally, in this section we present comparisons between the analyses and the numerical results. In Fig. 5 the analytical expressions Eqs. (8) and (12) are compared with numerical results. The threshold value for the breather- $k\bar{k}$ conversion is seen to depend strongly on the initial phase of the breather. None of the analyses take the initial phase [resulting in an initial energy different from Eq. (6)] into account. The influence of the initial phase for $\omega_B=0.6$ is shown in Fig. 6. The maximum discrepancy for $\theta=\omega_B t_0 \cong \pi/2$ is due to the fact that the breather initial energy deviates most from the energy of an unperturbed breather at this phase value.

IV. CONCLUDING REMARKS

In the present paper the influence of a driving force on a breather excitation is examined—large driving forces

cause the breather to split into a $k\bar{k}$ pair while for small driving forces the breather enters stationary modes. A perturbation method and a potential-energy argument yield expressions describing the threshold for breather decomposition. Numerical experiments show that the breather conversion depends strongly on the initial phase of the breather, thus the expressions only agree with the experiments in half the range of the initial phase. Inclusion of dissipation in the model will probably lead to damping of the stationary mode found for small driving

force values; however, we expect the break up into $k\bar{k}$ pairs for larger values of the driver to be qualitative similar to the one reported here.

ACKNOWLEDGMENTS

One of us (O.H.O.) thanks the Center for Nonlinear Studies for its hospitality. The work at Los Alamos was performed under the auspices of the U.S. Department of Energy.

*Permanent address: Niro Atomizer, Research and Development System and Design Division, Gladsaxevej, DK-2860 Soeborg, Denmark.

¹*Physics in One-Dimension*, edited by J. Bernasconi and T. Schneider (Springer, New York, 1981).

²N. F. Pedersen, *Solitons in Long Josephson Junctions*, in NATO Advanced Study Institutes Series, Proceedings of the 1982 Summerschool, Erice, Italy (Plenum, New York, 1983).

³E. Joergensen, V. P. Koshelets, R. Monaco, J. Mygind, M. R. Samuelsen, and M. Salerno, *Phys. Rev. Lett.* **49**, 1093 (1982).

⁴A. Barone, J. Esposito, C. J. Magee, and A. C. Scott, *Riv. Nuovo Cimento* **1**, 227 (1971).

⁵M. B. Fogel, S. E. Trullinger, A. R. Bishop, and J. A.

Krumhansl, *Phys. Rev. Lett.* **36**, 1411 (1976); **37**, 314 (1976); *Phys. Rev. B* **15**, 1578 (1977).

⁶D. J. Kaup and A. C. Newell, *Proc. R. Soc. London Ser. A* **361**, 413 (1978).

⁷D. W. McLaughlin and A. C. Scott, *Phys. Rev. A* **18**, 1652 (1978).

⁸A. C. Scott, *Phys. Scr.* **20**, 509 (1979).

⁹M. Inoue and S. G. Chung, *J. Phys. Soc. Jpn.* **46**, 1594 (1979).

¹⁰M. Inoue, *J. Phys. Soc. Jpn.* **47**, 1723 (1979).

¹¹P. S. Lomdahl, Ph.D. thesis, Technical University of Denmark, 1982, Report No. DCAMM-S20 (unpublished).

¹²O. H. Olsen and M. R. Samuelsen, *Phys. Rev. B* **28**, 210 (1983).